# Enhanced Instability in Thin Liquid Films by Improved Compatibility

Günter Reiter and Rajesh Khanna
*Institut de Chimie des Surfaces et Interfaces, CNRS, 15, rue Jean Starcky, BP 2488, 68057 Mulhouse Cedex, France*

Ashutosh Sharma
*Department of Chemical Engineering, Indian Institute of Technology at Kanpur, India 208 016*
(Received 6 March 2000)

We investigated experimentally the morphological evolution of thin polydimethylsiloxane films sandwiched between a silicon wafer and different bounding liquids with interfacial tensions varying by 2 orders of magnitude. It is shown that increasing the compatibility between film and bounding liquid by adding a few surfactant molecules results in a faster instability of shorter characteristic wavelength. Inversely, based on the characteristic parameters describing the instability we determined extremely small interfacial tensions with a remarkable accuracy.

PACS numbers: 47.20.–k, 68.10.–m, 68.15.+e, 68.55.–a

Thin liquid films sandwiched between a solid substrate and a bounding fluid are highly relevant in many scientific and technological processes such as adsorption, flotation, lubrication, and coatings. Attractive long-range interactions across the film may cause these films to become unstable and break up to form dry patches on the underlying substrate [1–17]. The interfacial tension ($\gamma_{fb}$) at the film-bounding fluid interface is a key parameter in the spatial and temporal evolution of this instability. Qualitatively, $\gamma_{fb}$ plays a purely stabilizing role before the appearance of dry patches or holes as it resists the deformation of the film surface. The higher $\gamma_{fb}$ is, the more difficult it is to rupture the film. This situation before the breakup of the film has to be contrasted to the subsequent dewetting. There, the interplay of three interfacial tensions (substrate-bounding fluid, substrate-film fluid, and film-bounding fluid), which determine the contact angle at the three phase contact line [18], affects the morphological evolution of the film, e.g., the growth of dry patches. In addition, the dewetting velocity is proportional to $\gamma_{fb}$. Quantitatively, linear theory as well as a dimensional analysis of the nonlinear governing equations predicts a linear dependence of length and time scales of the instability on the interfacial tension [19]. These theoretical results have never been verified or disproved experimentally. It has to be emphasized that varying $\gamma_{fb}$ by changing the bounding liquid affects, at the same time, the strength of the long-range interactions across the film [20]. Here, we avoided such a correlation by simply adding a few surfactant molecules to the bounding liquid. These surfactant molecules adsorbed at the interface between the film and the bounding fluid and thereby reduced $\gamma_{fb}$ without significantly changing the long-range interactions.

In the present experimental study we have chosen polydimethylsiloxane (PDMS) layers sandwiched between silicon wafers and aqueous surfactant solutions. The PDMS layer was a combination of a lower immobile monolayer which was chemically attached onto the wafer and an upper mobile spin casted thin film. This system offered many other advantages in addition to the excellent time resolution due to the slow evolution caused by the high viscosity and negligible loss of mass due to the low (zero) vapor pressure associated with polymer films. The immobile PDMS monolayer ensured that we never dewet the bare silicon wafer and that the bounding liquid does not creep below the PDMS layer to form an interface with the underlying silicon wafer [13]. This monolayer also allowed us to control the short-range interactions at the film-substrate interface. The stability of the PDMS layer in air, as indicated by the negative effective Hamaker constant for the silicon-PDMS-air system, allowed easy handling of the samples. The instability could be switched on by replacing air with water as the effective Hamaker constant then becomes positive [13,21]. Dilute aqueous solutions of different surfactants provided the possibility of changing interfacial tensions between the PDMS film and the liquid.

About 15 nm thick immobile PDMS layers were formed by chemically end grafting SiH monofunctionalized PDMS chains of uniform length (molecular weight, $M_w = 78k$, polydispersity, $I < 1.1$) on a previously cleaned silicon wafer [13]. The free PDMS film was formed on top of it by spin casting dilute solutions of nonreactive PDMS. Such films were stable in air and stayed smooth even after months of storage in air. The PDMS films were then covered by a small (about 10 $\mu$l) liquid droplet. Four different liquids that have a widely different degree of compatibility with PDMS (as expressed by the interfacial tension between the liquid and PDMS) were used for experiments: pure water (PW), ethylene glycol (EG), aqueous solutions of surfactant L77 (polyalkyleneoxide modified heptamethyltrisiloxane), and a short ($M_w = 3k$) water soluble diblock (80/20) copolymer PDMS-PEO (PP). The concentrations of aqueous solutions were about 5 times the critical micellar concentration, in absolute terms the concentration was 0.000 25 v/v for L77 and 0.01 v/v for PP, respectively. At such concentrations the film-bounding fluid interface had a constant surfactant concentration and none or negligible

 0031-9007/00/85(7)/1432(4)$15.00 

Marangoni flow induced complications were expected in the experiments [22,23]. The spatiotemporal evolution of the instability in PDMS films was followed at room temperature in real time by optical microscopy.

The interfacial tension for different liquids, PW, EG, L77, and PP, was estimated by applying the Young's equation [18] to a liquid drop on the PDMS film in air.

$$\gamma_{\text{PDMS-liquid}} = \gamma_{\text{PDMS-air}} - \gamma_{\text{liquid-air}} \cos\theta , \quad (1)$$

where $\theta$ is the equilibrium contact angle of the drop and $\gamma_{i-j}$ is the interfacial tension at the interface between species $i$ and $j$. $\theta$ was measured using a contact angle goniometer and the surface tension of the liquids and PDMS was measured using the Wilhelmy plate apparatus. $\gamma_{\text{PDMS-air}}$ was taken from literature as $20.8 \pm 0.1$ mN/m [24]. The results of the interfacial tensions are presented in Table I.

Figure 1 presents optical micrographs of the decomposition of a 60 nm thick film under different liquids to highlight the widely different "strengths" of the instability as the interfacial tension is changed. The evolution follows the characteristic path of spinodal dewetting of thin films [5,8,9,15]. Though the evolution is qualitatively similar for the three liquids, the time and length scales of the evolution are very different. A lowering of the interfacial tension by a factor of about 100 leads to about a hundredfold increase in the number of holes. By "holes" we mean isolated depressions which have reached the maximum depth. These holes then grow in size laterally with time. It is quite clear now that the instability is the strongest in series $C$ (L77, lowest $\gamma_{fb}$) and is the weakest in series $A$ (PW, highest $\gamma_{fb}$). As the results are shown for the same film thickness and the bounding liquids differ by only a small concentration of the surfactant, it is reasonable to assume (and will be shown later) that the excess intermolecular force field, e.g., due to van der Waals forces, is the same for the three cases. Thus, the increased compatibility or reduced interfacial tension between the film and bounding liquid results in an enhanced instability, i.e., a faster and more dense breakup of the film.

Having confirmed the qualitative trends of the effect caused by increased compatibility, we now proceed to quantify it. In order to isolate the effect of interfacial tension, the length scales at similar stages (not absolute times) of evolution should be compared. Note that the coalescence of holes increases the length scales (compare frames $A1$ and $A3$). The maximum number of holes per unit area ($N_{\max}$) will not have such add-on effects. As expected [5], $N_{\max}$ is found to be directly related to the characteristic spinodal wavelength ($\lambda$; see Fig. 2). Thus, $N_{\max}$ can be attributed to changes in interfacial tension only. In addition, Fig. 2 also shows that $\lambda$ stays rather constant, as expected in spinodal dewetting of thin films [5,8,9,15], before $N_{\max}$ is reached at time $\tau$: $q(t < \tau) = 2\pi/\lambda = 2\pi(N_{\max})^{1/2}$.

Figure 3 presents the variation of $N_{\max}$ with the PDMS layer thickness ($h$) for different interfacial tensions. Based on hundreds of similar experiments, the following general observations can be drawn: $N_{\max}$ increased rapidly with the decreasing film thickness. For any given thickness, L77 and PW resulted in the maximum and minimum densities of holes, respectively. The results for PP are intermediate and those of EG are very similar to that of water. The

TABLE I. Characteristic interfacial parameters for the liquids used.

| Liquid (b) | $\gamma_{\text{liquid-air}}$ [mN/m] | $\theta$ [deg] | $\gamma_{\text{PDMS-liquid}}$ [mN/m] |
|---|---|---|---|
| PW | $72.8 \pm 0.2$ | $104 \pm 1$ | $38.4 \pm 3\%$ |
| EG | $38.3 \pm 0.2$ | $86 \pm 1$ | $18.1 \pm 5\%$ |
| PP | $23.3 \pm 0.2$ | $57 \pm 2$ | $8.1 \pm 7\%$ |
| L77 | $21.5 \pm 0.1$ | $17 \pm 1$ | $0.3 \pm 33\%$ |

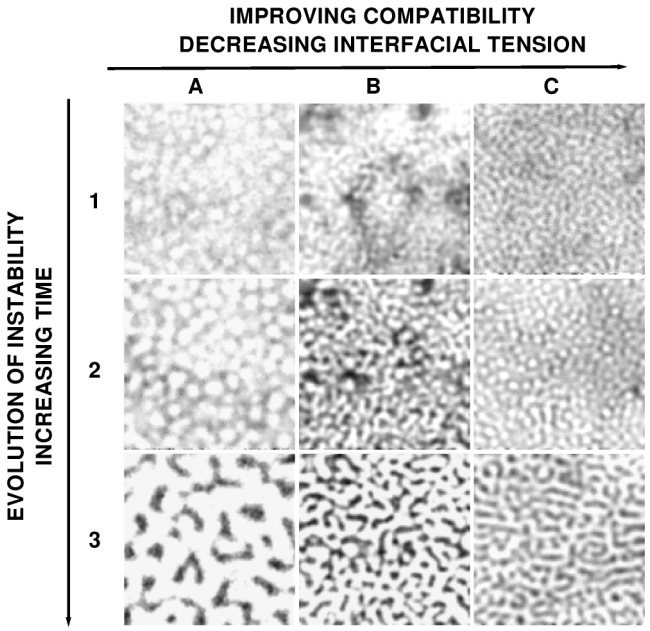


FIG. 1. Changes in the length and time scales of breakup of a 60 nm thick PDMS film under bounding liquids which have a varying level of compatibility with PDMS. The interfacial tensions change from $38.4 \pm 3\%$ mN/m in series $A$ (pure water) to $8.1 \pm 8\%$ mN/m in series $B$ (PP) and then finally to $0.3 \pm 33\%$ mN/m in series $C$ (L77). The increasing levels of gray denote thicker portions. In each series the evolution is shown by three (1, 2, and 3) representative snapshots to mark the different stages of evolution of instability. The actual times in seconds for series $A$, $B$, and $C$ are (25, 65, and 200), (15, 45, and 100) and (5, 10, and 15), respectively. The area shown in frames of series $A$ and $B$ is $100 \times 100$ $\mu$m$^2$. For the purpose of clarity the results for series $C$ are shown in an area which is 16 times smaller ($25 \times 25$ $\mu$m$^2$). A rather smooth surface of the film evolves into a collection of circular depressions (frames $A1$, $B1$, and $C1$). These shallow depressions develop into circular holes (frames $A2$, $B2$, and $C2$) which grow laterally to coalesce with other growing holes and form long cylindrical ridges (frames $A3$, $B3$, and $C3$) which break up into small drops later on. The maximum number of holes in $100 \times 100$ $\mu$m$^2$ is about 60, 300, and 6000 for PW, PP, and L77, respectively.

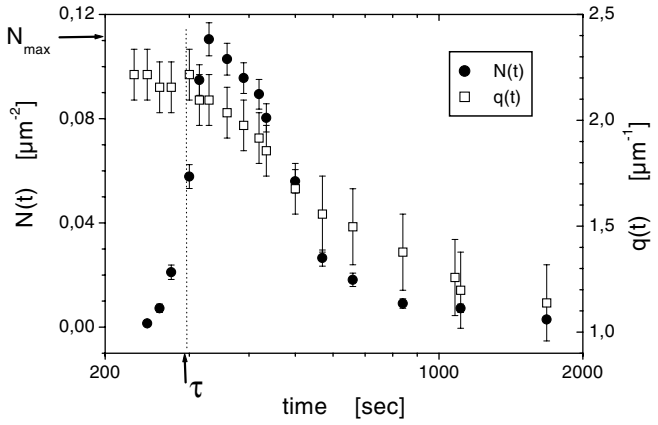


FIG. 2. Temporal evolution of the number of circular full thickness depressions $N(t)$ and the characteristic wave vector $q(t)$ obtained from a 2D Fourier transform ($q = 2\pi/\lambda$; $\lambda$ is the characteristic distance between depressions). The initial film thickness was 105 nm. The bounding liquid was L77 aqueous solution. $\tau$ defines the characteristic time for the appearance of holes. $N_{\max}$ represents the maximum number of holes.

relative densities of holes among different liquids for any given $h$ are largely invariant of $h$. There is an inverse power law dependence of $N_{\max}$ on $h$ as shown by the dotted straight lines which adequately represent the data on a double logarithmic plot. It is also clear that the exponent of the power law is similar for different liquids.

We averaged these results, to obtain a higher accuracy, by fitting straight lines of fixed slope $-4$ to the data for individual liquids. A slope of $-4$ is very similar to that given by the best fitted values for the different liquids which are $-4 \pm 0.3$, $-3.7 \pm 0.1$, $-4.4 \pm 0.5$, and $-3.6 \pm 0.4$ for the cases of L77, PP, PW, and EG, respectively. A slope of $-4$ is also in accordance with our earlier reported work on similar samples [13]. It is worthwhile to recall at this point

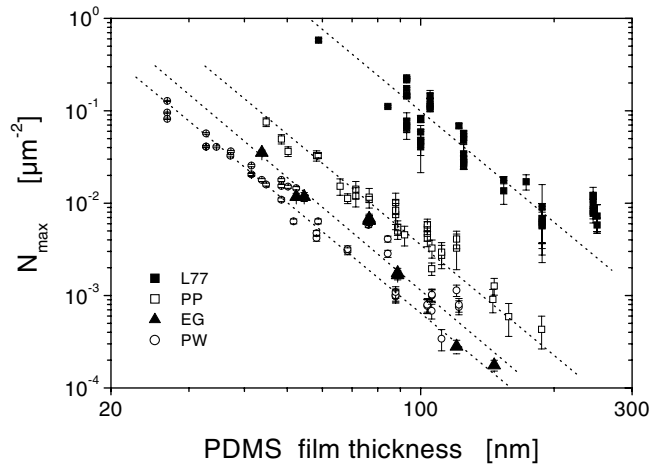


FIG. 3. The variation of maximum number density of holes with film thickness for different bounding liquids. Results are presented for the four liquids which have a varying level of compatibility with PDMS: PW (open circles), PP (open squares), L77 (filled squares), and EG (filled triangles).

that a slope of $-4$ strongly suggests that the instability is engendered by long-range van der Waals (vdW) interactions. According to the theoretical model for instability engendered by vdW forces, $N_{\max}$ is given by [1–5,19]

$$N_{\max} = A_{sfb}/(16\pi^3\gamma_{fb}h^4) = Ch^{-4}, \qquad (2)$$

where $A_{sfb}$ is the effective Hamaker constant for the system silicon-PDMS-liquid. Equation (2) clearly shows that $N_{\max}$ is directly proportional to $A_{sfb}$ and inversely proportional to $\gamma_{fb}$ and $h^4$. In Table II we have normalized $\gamma_{fb}$ and $N_{\max}$ with respect to the values for PW to highlight the relative enhancement of the instability. We find that for PW, PP, and L77 the relative hole density is inversely proportional to the relative interfacial tensions. The large error bar in the relative interfacial tension in the case of L77 is a propagation of uncertainty in the initial measurement of $\gamma_{fb}$. The deviation of data for EG from this inverse dependence is expected as the excess intermolecular force field strength has to be different to that in the case of aqueous solutions. To further prove this, we calculated the Hamaker constants by using Eq. (2) and the measured values of $\gamma_{fb}$ for different liquids. Two important conclusions can be drawn from the results shown in Table II. The addition of a few surfactant molecules results in the same Hamaker constant which is, however, 2 to 3 orders of magnitude higher than what is expected based on the assumption of additive contribution of dispersive forces of the individual media, a further confirmation of previous results [8,9,21,25].

As an additional feature of these experiments we now present a new approach to estimate the interfacial tension. The standard methods suffer from large uncertainties when the interfacial tensions are very low (refer to the L77 case). We can apply the theoretical model of spinodal decomposition to back calculate the interfacial tension from the characteristic length AND time scales of the instability. To highlight the robustness of the method we apply it for a general form of intermolecular potential which can have *any arbitrary* dependence on the film thickness. For a *general* form of potential, $N_{\max}$, and $\tau$ are given by [4,5,19]

$$N_{\max} = P/(8\pi^2\gamma_{fb}), \qquad (3)$$

$$\tau \approx 12\eta\gamma_{fb}/(h^3P^2), \qquad (4)$$

where $P$ is the force per unit volume at the initial film thickness and $\eta$ is the viscosity of the film liquid (PDMS).

TABLE II. Results obtained from the analysis of Fig. 3.

| Liquid (b) | $\frac{\gamma_{\text{PDMS-PW}}}{\gamma_{\text{PDMS-}b}}$ | $\frac{(N_{\max})_b}{(N_{\max})_{\text{PW}}}$ | $A_{sfb}$ [$10^{-18}$ J] |
|---|---|---|---|
| PW | 1 | 1 | 1.8 ± 10% |
| EG | 2.1 ± 10% | 1.4 ± 2.5% | 1.2 ± 15% |
| PP | 4.7 ± 10% | 4.6 ± 15% | 1.8 ± 10% |
| L77 | 128 ± 40% | 96 ± 20% | 1.4 ± 40% |

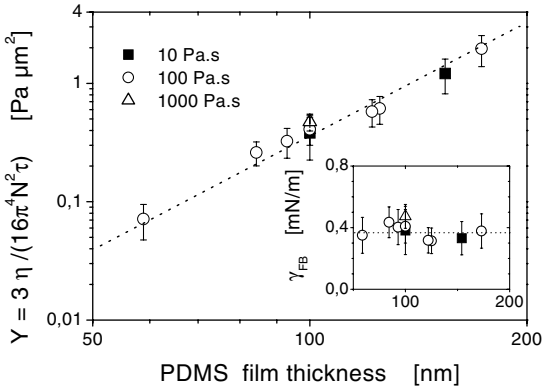


FIG. 4. Double logarithmic plot of variation of the parameter $Y$ (see text) with PDMS film thickness for L77 as the bounding fluid. A straight line of slope 3 adequately describes the data. The inset shows the interfacial tension $\gamma_{fb}$ with PDMS film thickness with the straight line representing the mean value. The different symbols represent different film viscosities.

Please note that Eq. (2) is a special form of Eq. (3) for the case of vdW interactions. After eliminating $P$ from Eqs. (3) and (4) one obtains

$$Y = 3\eta/(16\pi^4 N_{\max}^2 \tau) = \gamma_{fb} h^3. \quad (5)$$

As $N_{\max}$, $\tau$, and $h$ were measured independently, $\gamma_{fb}$ can be calculated using Eq. (5). Figure 4 presents the variation of the parameter $Y$ with $h$ for L77 from which $\gamma_{fb}$ comes out to be $0.38 \pm 0.05$ mN/m. Apart from providing a simple and reliable method to obtain the interfacial tension this stringent test of self-consistency of both length AND time scales with film thickness, interfacial tension, and viscosity for ANY form of potential in the spinodal dewetting model also substantiates our belief that spinodal decomposition is at work in these systems. The unexpectedly high strength of these forces still remains an unsolved question and needs to be pursued.

We summarize by saying that the present experimental results strongly corroborate the theoretical relationship between the interfacial tension and the strength of instability in thin liquid films. A lowering of interfacial tension results in a much stronger instability. For very low values of $\gamma_{fb}$, as in the case of L77, even several hundred nanometer thick films could be ruptured in seconds. Furthermore, based on a self-consistency test for the spinodal decomposition mechanism, we illustrate a simple method to measure interfacial tensions which is specially suitable for measuring very low values. This self-consistency also vindicates the theory of thin film breakup.

We are indebted to Philippe Auroy for providing us with the end functionalized PDMS molecules. Fruitful discussions with Alain Casoli, Philippe Auroy, Marie-Odile David, and Françoise Brochard and help provided by Hamidou Haidara and Laurent Vonna are gratefully acknowledged. This work was supported by the Indo-French Centre for the Promotion of Advanced Research/Centre Franco-Indien Pour la Promotion de la Recherche.

[1] A. Vrij, Discuss. Faraday Soc. **42**, 23 (1966).
[2] M. B. Williams and S. H. Davis, J. Colloid Interface Sci. **90**, 220 (1982).
[3] F. Brochard-Wyart and J. Daillant, Can. J. Phys. **68**, 1084 (1990).
[4] A. Sharma, Langmuir **9**, 861 (1993); **9**, 3580 (1993).
[5] A. Sharma and R. Khanna, Phys. Rev. Lett. **81**, 3463 (1998).
[6] G. Reiter, Phys. Rev. Lett. **68**, 75 (1992).
[7] M. Sferrazza, M. Heppenstall-Butler, R. Cubitt, D. Bucknall, J. Webster, and R. A. L. Jones, Phys. Rev. Lett. **81**, 5173 (1998).
[8] R. Xie *et al.,* Phys. Rev. Lett. **81**, 1251 (1998).
[9] S. Herminghaus *et al.,* Science **282**, 916 (1998).
[10] T. G. Stange, D. F. Evans, and W. A. Hendrikson, Langmuir **13**, 4459 (1997).
[11] K. Jacobs, S. Herminghaus, and K. R. Mecke, Langmuir **14**, 965 (1998).
[12] U. Thiele, M. Mertig, and W. Pompe, Phys. Rev. Lett. **80**, 2869 (1998).
[13] G. Reiter *et al.,* Europhys. Lett. **46**, 512 (1999); Langmuir **15**, 2551 (1999).
[14] R. A. Segalman and P. F. Green, Macromolecules **32**, 801 (1999).
[15] G. Reiter, Science **282**, 888 (1998).
[16] S. Herminghaus, Phys. Rev. Lett. **83**, 2359 (1999).
[17] R. Yerushalmi-Rozen, T. Kerle, and J. Klein, Science **285**, 1254 (1999).
[18] P. G. De Gennes, Rev. Mod. Phys. **57**, 827 (1985).
[19] R. Khanna and A. Sharma, J. Colloid Interface Sci. **195**, 42 (1997).
[20] J. Visser, J. Adv. Colloid Interface Sci. **3**, 331 (1972).
[21] G. Reiter *et al.,* J. Colloid Interface Sci. **214**, 126 (1999).
[22] A. De Wit, D. Gallez, and C. I. Christov, Phys. Fluids **6**, 3256 (1994).
[23] A. Sharma and E. Ruckenstein, J. Colloid Interface Sci. **111**, 8 (1986); **113**, 456 (1986).
[24] B. B. Sauer and G. T. Dee, Macromolecules **24**, 2124 (1991).
[25] W. Zhao *et al.,* Phys. Rev. Lett. **70**, 1453 (1993).